JOURNAL OF MATERIALS SCIENCE 31 (1996) 5399–5407

The effect of fibre orientation of the dry sliding wear of borsic-reinforced 2014 aluminium alloy

Y. SAHIN
Department of Technical Education, Gazi University, Ankara, Turkey
S. MURPHY
Department of Mechanical & Electrical Engineering, Aston University, Birmingham, UK

The effect of fibre orientation on the dry sliding wear of continuous B(SiC) fibre reinforced aluminium alloy composites was investigated using a pin-on-disc wear testing machine. The metal–matrix composites (MMC) samples were tested in the normal (N), parallel (P) and antiparallel (AP) orientations sliding against a steel counter disc at a fixed speed of 1 m s^{-1} under loads of from 12 to 60 N.

The results showed that for the matrix alloy and MMCs, the average wear increased linearly with load. Wear of the MMCs was insensitive to fibre content but for composites with fibre contents at or above the minimum of 16 vol% used for this work, the wear rate was about 18% of that of the unreinforced matrix. Fibre orientation had a minor effect on wear rate; the N orientation gave the lowest wear rate with the AP orientation slightly higher and the P orientation significantly higher.

The average coefficients of friction of the MMCs in N and AP orientations decreased linearly with increased wear rate and non-linearly with increased load, but the P orientation was insensitive to either variable.

It was concluded from these results and a metallographic examination that the mechanism of wear of MMCs was essentially oxidative wear of the matrix. The hard fibres modified this to slightly different degrees depending on their orientation relative to the wear surface and sliding direction.

1. Introduction

It is well known that metal–matrix composites (MMCs) are superior in certain respects to the common engineering metals and alloys, and advantages exist in combinations of such properties as low thermal expansion, high specific strength, high specific stiffness and resistance to creep deformation at high temperatures. Due to this, MMCs are being used extensively today for the aerospace and more recently automobile industries [1–6]. By reinforcing aluminium with silicon carbide-coated boron fibres, which we shall refer to as B(SiC), or other fibres, it has been possible to develop composites whose mechanical properties can be compared favourably with those of conventional alloys [7].

In a recent investigation the wear characteristics of B(SiC)/2014 aluminium alloy composites were compared with those of the aluminium alloy matrix. It was shown that the adhesion or delamination theories of wear could explain the behaviour of the matrix while fibres were worn down by chipping of protruding fibre ends when the wear surface was normal to the fibre axes [8]. However, in the last few years studies on friction and wear have been focused on graphite fibre-reinforced composites, and the orientation of the fibres with respect to the sliding surface has been found to be the most important parameter in determining the wear rate and coefficient of friction of a number of MMCs. For example, Eliezer *et al.* found that in graphite/bronze MMCs the composite had a lower wear rate when the fibres were orientated normal to the wear surface than when the fibres were parallel [9]. Amatea *et al.* could find no significant effect of fibre orientation on the wear of a graphite-reinforced aluminium alloy MMC [10], although later it was reported that a thick layer of graphite debris had masked any fibre orientation effect, and in composites with a thinner layer strongly anisotropic wear behaviour was observed, the normal (N) and parallel (P) orientations having the lowest and highest wear rates respectively [11]. More recently the same investigators found that wear rate was dependent on the type of carbon fibre used in the composites, for low-modulus polyacronitrile precursor (PAN) carbon fibres gave a better wear resistance than high-modulus rayon or PAN based fibres [12]. Saka *et al.* found that stainless steel wires in the P orientation in an aluminium alloy matrix gave a lower composite wear rate than those in the N orientation, and the same workers showed that in a graphite/aluminium alloy MMC the

0022–2461

N orientation gave a lower wear rate than either the P or AP orientations, where P represents fibres parallel to the sliding surface, with the sliding direction parallel to the fibre axis, and AP represents a similar orientation of the plane but the sliding direction normal to the fibre axis [13]. In contradiction to this result, another study showed than in a carbon/zinc alloy MMC the AP orientation gave the lowest wear rate, due to the lubricating action of the carbon and the presence of chopped fibres on the wear surface [14].

In view of these uncertainties, this study set out to determine the effects of fibre orientation on the wear rate and friction of a series of B(SiC)/2014 alloy unidirectional fibre MMCs with different fibre contents, and to determine the mechanisms of wear.

2. Experimental work

2.1. Materials

The composites were made by a liquid metal infiltration process in which liquid aluminium alloy 2014 was injected into a heated die containing pre-placed parallel layers of continuous Borsic fibre tape. These fibres had an overall diameter of 140 mm which included a tungsten core 15 mm in diameter and a surface coating of silicon carbide 2.5 mm thick. The fibres had a tensile strength of 2.9 GPa and a modulus of elasticity of 400 GPa [15]. The plate-shaped samples made by infiltration contained 0, 16, 23, 27 and 32% by volume of fibres. The 23% plate, which was made for other purposes, differed slightly from the others in that it contained a very small number of fibres (of the order of 5%) placed transversely to the main group. The properties of the matrix alloy and MMCs are listed in Table I.

The MMC plates were cut into small cylinders for pin-on-disc wear testing using electrical discharge machining, to provide N, P and AP orientations on diametral planes. This was followed by polishing the flat ends with silicon carbide grinding paper. The cross-sectional area of the cylinders was 37.98 mm^2. The counterface material for the wear tests was a BS970 534A99 steel disc 120 mm diameter by 12 mm thick, which was heat-treated to give a surface hardness of 59–63 Rc and ground to a surface finish of approximately 0.15 mm centre-line-average (CLA).

2.2. Testing procedure

The materials were tested in the N, P and AP orientations. The wear pin specimens made from the MMC in these orientations were approximately 4.5 mm in length and 6.33 mm in diameter, too short to fit into a standard pin-on-disc machine. To form a pin of the necessary length the cylinders were bonded to a 50 mm long steel extension pin of the same diameter using an epoxy adhesive, with a brass sleeve fitted over the joint for extra strength. The pin was then mounted in a brass holder in the wear testing machine so that it was held firmly perpendicular to the flat surface of the rotating counter disc. The rubbing surface of the pin was prepared to a standard fine finish by fixing silicon carbide papers of successively finer grit sizes to a dummy disc and rotating the disc with the pin pressed lightly against it. This lapped the pin surface to the disc and gave a similar surface finish to each pin tested. The pin and the counter disc were ultrasonically cleaned to remove any contaminating material and the pin was weighed before the start of each test. In a series of dry sliding wear tests at initially ambient temperatures, loads of 12, 24, 44 or 60 N were applied to the pin and the tests were carried out at a sliding speed of 1.0 $m\,s^{-1}$ for a total sliding distance of 7.2 km. The frictional force was continuously monitored by measuring the deflection of a beam by means of a load-calibrated strain gauge transducer. The axial displacement of the pin due to wear was also monitored by another displacement transducer, but the wear volume was measured by cleaning the pin with acetone and re-weighing it at the conclusion of the test, using the measured density of the MMC to calculate the wear rate in terms of volume lost per unit sliding distance. Each test was repeated six times and the results averaged.

2.3. Scanning electron microscopy

To investigate the wear mechanisms involved, the worn surfaces and sections perpendicular to the wear surfaces of each type of wear sample were examined in a scanning electron microscope (SEM) in secondary electron (SE) and back-scattered electron (BSE) contrast imaging. Wear surfaces were gold-coated before examination, sections were prepared to a 1 μm surface finish by standard metallographic techniques and examined in the as-polished state.

3. Results

3.1. Wear rate

The average volumetric wear rates for N, P and AP orientations were determined, and are illustrated graphically in Fig. 1(a) to (d) as a function of fibre content at different loads. The tests shown in these figures were carried out at a sliding speed of 1 $m\,s^{-1}$ at the indicated loads.

TABLE I Properties of unidirectional B(SiC)-reinforced aluminium matrix composite and unreinforced matrix

Type of tested materials	Volume fraction of fibre (%)	Density ($kg\,m^{-3}$)	Hardness (BHN)	Tensile strength (MPa)
2014 Al-alloy matrix	0	2789	87	172
B(SiC)/Al composite	16	2760	220	312
B(SiC)/Al composite	23	2740	212	235
B(SiC)/Al composite	27	2727	343	445
B(SiC)/Al composite	32	2720	424	524

Fig. 1 shows that the wear rate of the matrix increased sharply with load, but that the addition of fibres to the matrix greatly reduced the wear rate. An increase in the volume of fibres beyond 16% produced a small decrease in wear rate, but in general wear was then insensitive to fibre content to the maximum content of 32%.

3.2. Friction

Coefficients of friction were calculated from the measured frictional forces and pin end loads, and the average values are plotted as a function of fibre volume in Fig. 2(a) to (d). These graphs showed that the coefficient of friction of the matrix alloy decreased very slightly with load from 0.4 at 12 N to 0.31 to 44 N, but

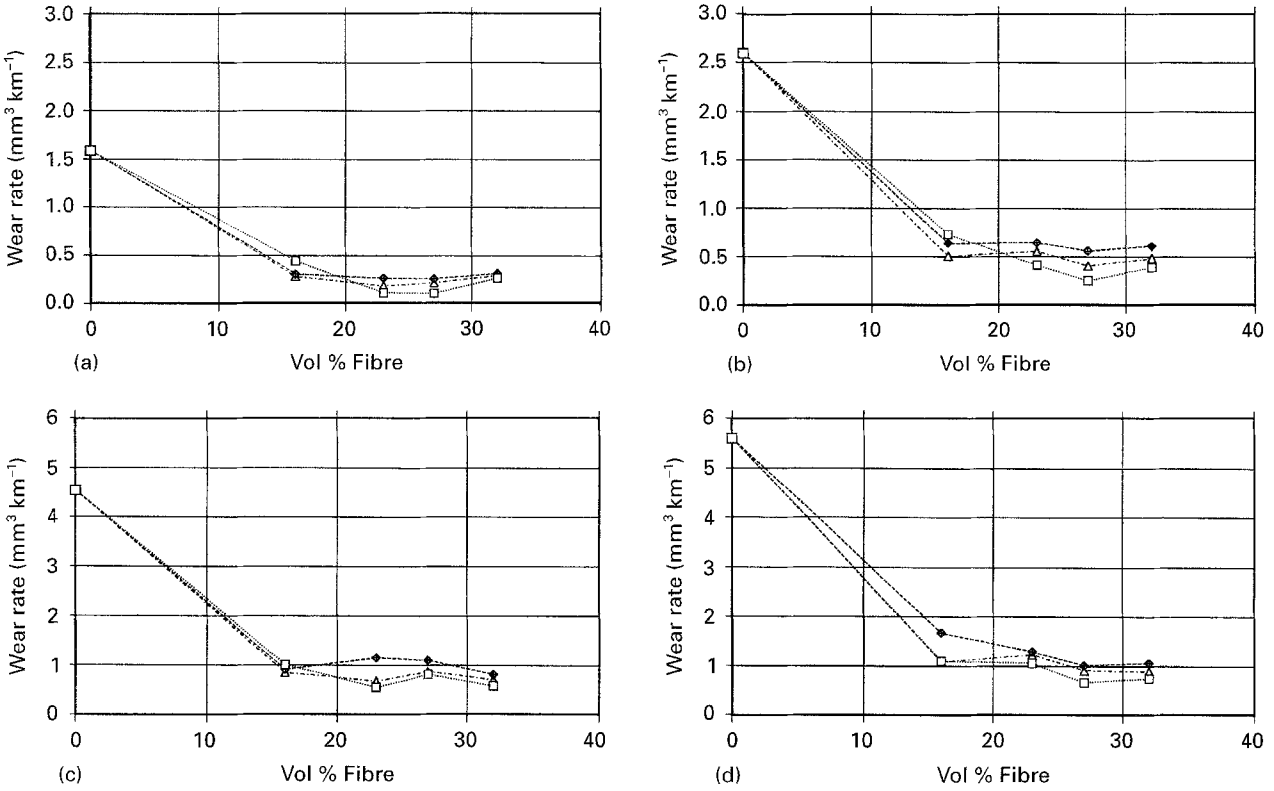

Figure 1 Average volumetric wear rates for N (□), P (◇) and AP (△) orientations as a function of fibre content at loads of (a) 12 N, (b) 24 N, (c) 44 N, (d) 60 N.

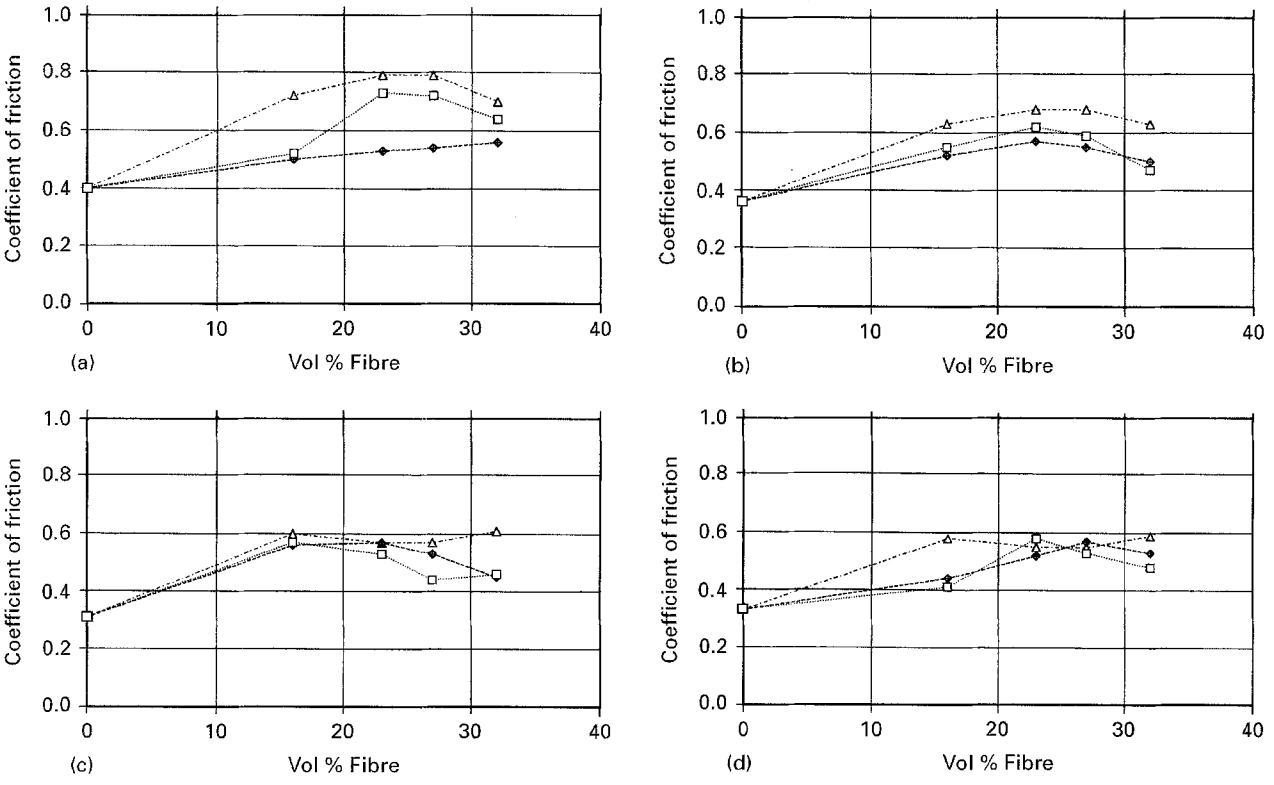

Figure 2 Average coefficient of friction as a function of fibre volume at loads of (a) 12 N, (b) 24 N, (c) 44 N, (d) 60 N. □ N; ◇ P; △ AP.

then increased slightly. The coefficients of friction of the composites were generally much larger than that of the unreinforced matrix alloy but varied substantially with fibre volume and load.

3.3. Surface and subsurface observations

The worn ends of some of the wear pins were cut off and examined in the SEM in order to study the morphology of the wear surfaces at high resolution.

One of the N orientation surfaces is shown in SE imaging mode in Fig. 3. The pin was from a 32% fibre composite, tested at 44 N corresponding to a high load – low wear rate condition. The surface had a relatively smooth surface at this low magnification, in spite of the high load. Compared with the unreinforced matrix there was a much reduced amount of plastic deformation, but there was some smearing of the matrix over the protruding ends of the fibres. Fig. 4 shows the same surface at higher magnification, and revealed that the exposed ends of the B(SiC) fibres had been chipped at the edges during the wear test. The maximum length of the chipped regions on the fibres was about 25 μm, but the size varied from place to place. Few of the fibre fragments had become embedded in the wear surface after detachment.

Fig. 5 shows the surface of another 32% fibre pin tested in the P orientation under a load of 24 N and imaged in SE mode. This low magnification micrograph showed that large pieces of fibre, partially exposed by wear, had peeled away from the surface under this modest load, leaving deep hollows in the surface. In a BSE image of the same part of the surface (Fig. 6), atomic number contrast showed clearly the fracture and removal of large sections of the tungsten-cored boron fibres with relatively few fibre particles embedded in the wear surface. At higher magnification (Fig. 7) shattering of the exposed fibres and partial filling of the hollows left by fibre removal is evident in this SE micrograph. Fig. 8 is a low magnification micrograph of another P orientation test pin containing 27% fibre, tested at the same load but the lower speed of 0.6 $m\,s^{-1}$, and this shows that some pieces of fibres had been pulled bodily out of the surface by the axial frictional forces.

A significantly different situation was revealed by examination of the AP orientation pins. Fig. 9 shows an SE micrograph of a 27% fibre pin tested under a 24 N load at 1.0 $m\,s^{-1}$ in the AP orientation. Sliding transverse to the fibre axes had subjected the exposed fibres to large bending moments and this had caused intense fragmentation of the fibres and only modest grooving of the surface in the rubbing direction. A notable feature was that the hollows left by detachment

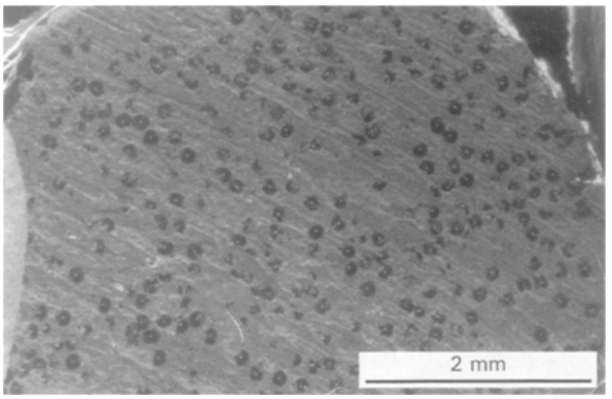

Figure 3 SE image of a worn surface of B(SiC)-reinforced MMC pin tested in the N-orientation at 1.0 $m\,s^{-1}$ speed and 44 N load, showing relatively smooth surface, leading edge to left. ($Vf = 32\%$).

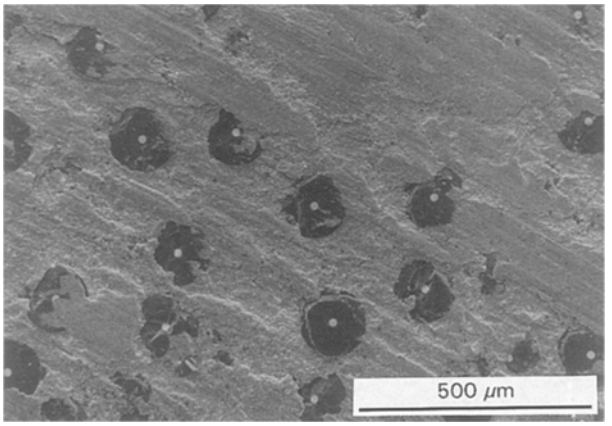

Figure 4 Increased magnification of Fig. 3, showing matrix smearing over the fibre ends and chipping of the fibre edges.

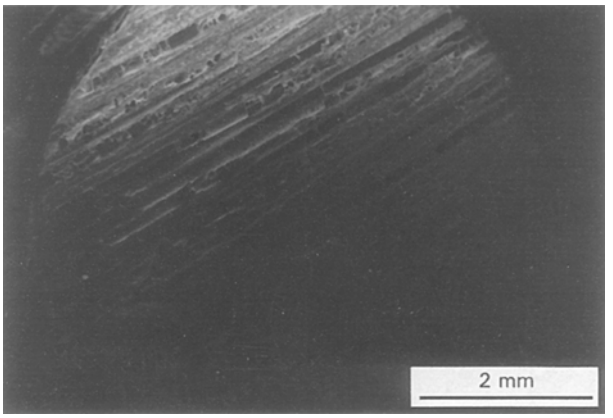

Figure 5 SE image of a worn surface of a B(SiC)-reinforced MMC pin tested in the P-orientation at a speed of 1.0 $m\,s^{-1}$ and 24 N load, showing peeling of fibres, leading edge upper right. ($Vf = 32\%$).

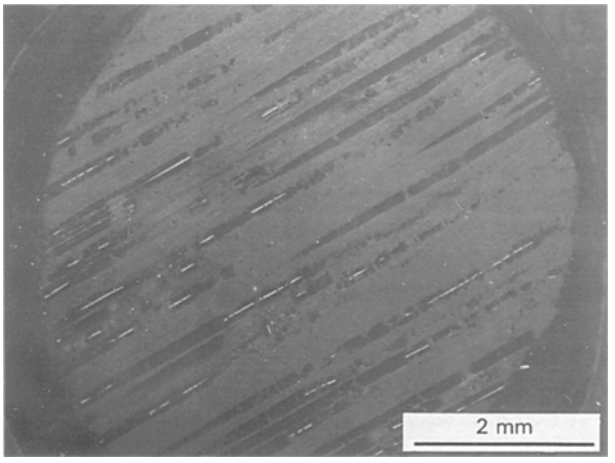

Figure 6 BSE image of the same sample of Fig. 5, showing fracture of boron fibres and their tungsten cores.

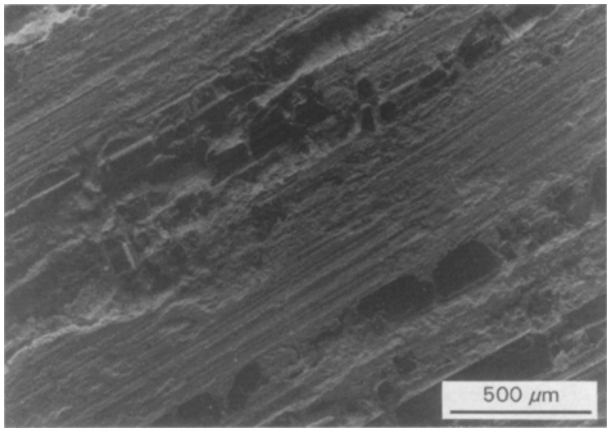

Figure 7 Increased magnification SE image of the worn surface of the MMC pin tested at a speed of 1.0 m s^{-1} and 24 N load, showing the cracking and displacement of fibres, leading edge to left.

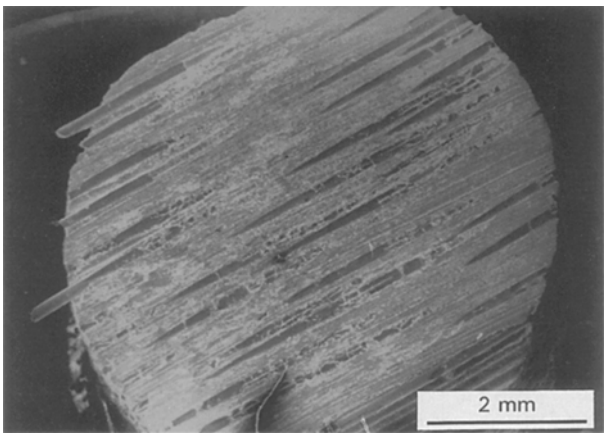

Figure 8 SE micrograph of the worn surface of the MMC pin, tested in the P-orientation, at a speed of 0.6 m s^{-1} and 24 N load, showing broken and pulled-out fibres, leading edge to right. ($Vf = 27\%$).

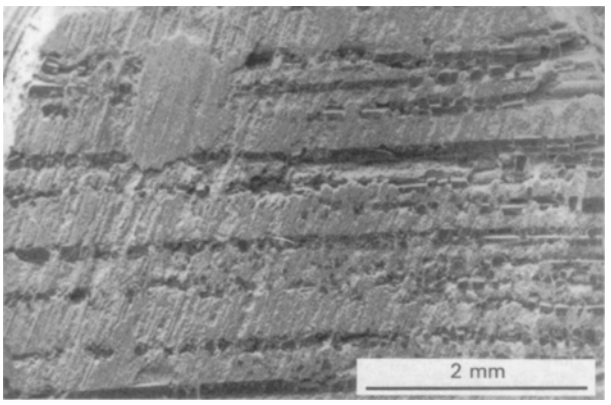

Figure 9 SE image of a worn surface of the MMC pin, tested in the AP-orientation, at a speed of 1.0 m s^{-1} and 24 N load, showing fibre bending, fibre fracture and fibre removal from the place, leading edge at bottom. ($Vf = 27\%$).

of pieces of fibre had been filled by wear debris. When the same area was examined in BSE mode (Fig. 10), the atomic number contrast confirmed that many pieces of fibre had been retained on the wear surface.

Sections through the wear surfaces on a plane transverse to the sliding direction were examined in the SEM to determine the nature and depth of any surface damage caused by dry wear. Fig. 11 shows such a section of a 27% fibre pin tested in the N orientation and imaged in SE mode at high magnification. In this micrograph a fibre lying normal to the surface was sectioned at a shallow angle. The boron core (dark) is to the right and the silicon carbide coating (grey) is in the middle with the matrix to the left; fracture of the boron has occurred resulting in partial removal of a chip 20 to 25 μm long, and a layer of wear debris about 10 μm deep has been deposited on the surface of the fibre.

Fig. 12 shows a section through a P-orientation pin surface containing 27% fibre, tested at a load of 44 N. Partial fracture of a fibre below the surface had caused the formation of splinters which remained *in situ*, which ranged in size from 30 to 60 μm, and the matrix alloy was deformed and cracked to a depth of 40 to 60 μm. The BSE image of the same area shown in Fig. 13 shows more clearly the deformed layer under the wear track and the presence of many oxide debris particles embedded in a shallow wear groove in the surface.

Fig. 14 shows a section through an AP-orientation 27% volume fibre pin surface, tested at 44 N which shows a fractured fibre lying in the surface, and very

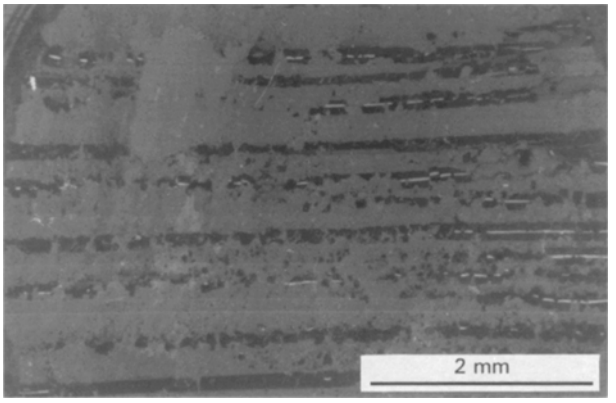

Figure 10 BSE image of Fig. 9, showing pulled-out fractured fibres embedded in the matrix.

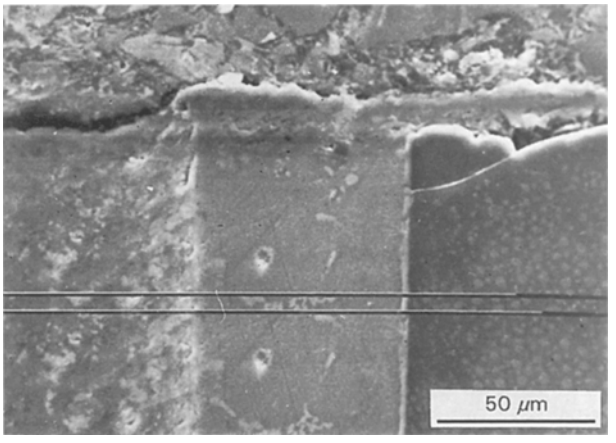

Figure 11 SE micrograph of section through the wear surface of an N-orientation MMC pin sectioned normal to the sliding direction at a speed of 1.0 m s^{-1} and 44 N load, showing fracture of the fibre end, deformed and smeared matrix at the surface. ($Vf = 27\%$).

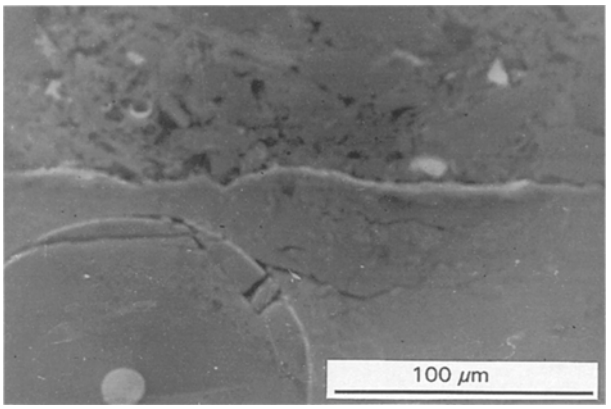

Figure 12 SE micrograph of section through the wear surface of a P-orientation MMC pin sectioned normal to the sliding direction, tested at a speed of 1.0 m s^{-1} and 44 N load, showing subsurface plastic deformation and cracking. ($Vf = 27\%$).

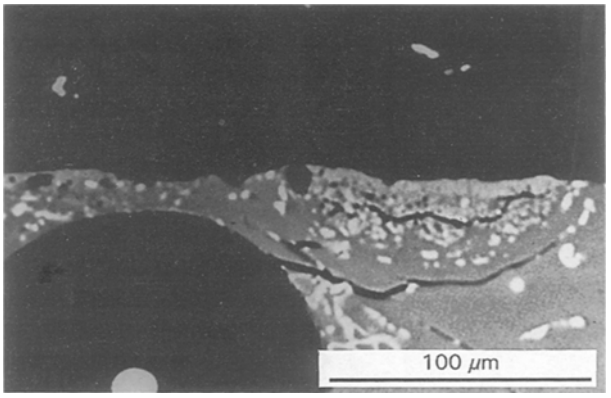

Figure 13 BSE image of the same sample as Fig. 12, showing deformed layer and cracks.

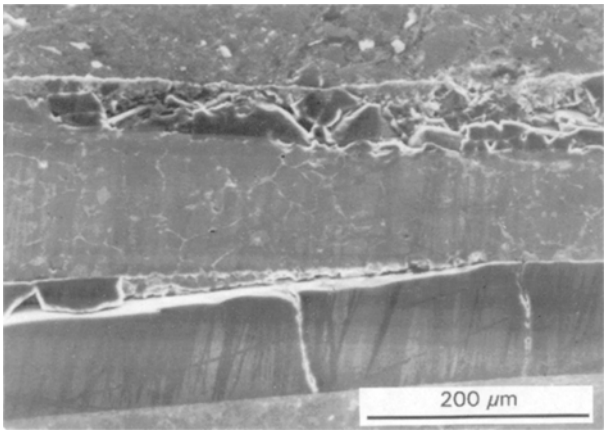

Figure 14 SE micrograph of section through the wear surface of an AP-orientation containing 27% fibre, showing extensively fractured fibres below the surface.

extensive damage to another fibre 200 μm below the surface. Fig. 15 shows extensive subsurface plastic deformation, delamination cracks and surface debris infilling wear grooves in a similar AP sample.

4. Discussion

Unlike carbon fibre-reinforced composites, the wear debris from boron does not form platelets which can act as a solid lubricant, and so the wear behaviour of our composites was uncomplicated by that peculiar feature. Thus the effects of fibre orientation relative to the sliding surface and sliding direction must reflect the situation for a wider range of MMC materials than those which contain boron fibres.

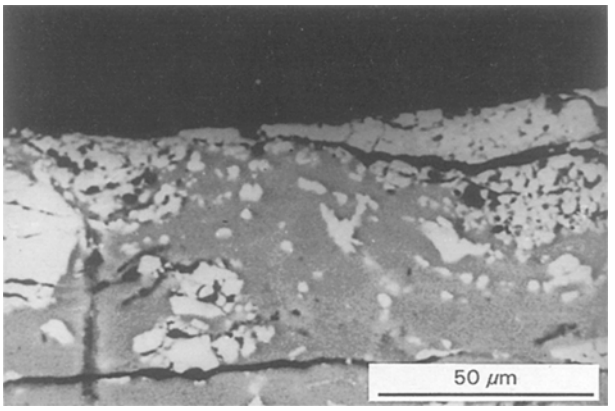

Figure 15 BSE image of section through the wear surface of a 27% fibre AP orientation pin at higher magnification, showing the deformation and cracking of the subsurface matrix.

Some immediate conclusions may be drawn from the wear rate curves shown in Fig. 1. It is clear from this figure that the unreinforced alloy wore much more rapidly than the reinforced materials, and comparison of the wear curves for different loads showed that for both unreinforced alloy and MMCs wear rates increased with load. A second clear result was that within the ranges studied, neither fibre content nor fibre orientation had a large effect on the wear rate of the composites. This being so the behaviour of the composites relative to the matrix alloy could be examined by calculating the "global average" wear rate of the composites, i.e. the average for all volume fractions and orientations, and comparing this with the wear rate of the unreinforced alloy. When these values were plotted against load it was found that both showed a linear dependence, as shown in Fig. 16. Although the rate of change for the composites was much smaller than that of the matrix, there was a close correlation between the wear rates at each load, the average wear rate of the composites being $18 \pm 2\%$ of that of the matrix at the same load. This finding suggests that the mechanism of wear is essentially similar for each class of material, the fibres modifying the wear process to reduce wear, but not changing it in essence.

This conclusion is supported by a comparison of the wear rate curves with the metallographic observations. Fig. 1 shows that in general the wear rate declined gently with increased volume fraction of fibre although the magnitude of the variation changed in an irregular manner and increases were observed in most cases at the highest fibre contents. While the latter point is not immediately explained, the general effect of fibres seems to be related to two effects: strengthening of the matrix and changing the sliding surface topography. In a previous study it was shown that for these composites hardness was a strong linear function of fibre volume fraction [8]. Since the wear rates shown in Fig. 1 were a much weaker function of fibre

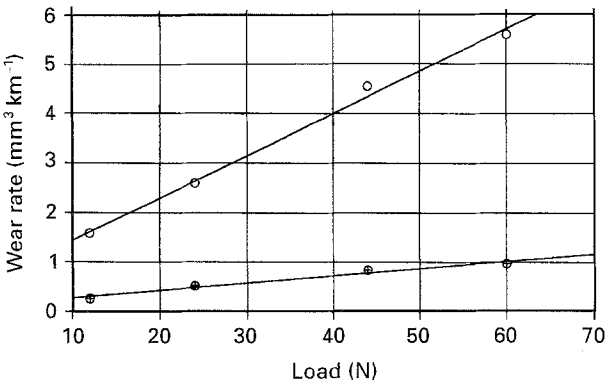

Figure 16 Average volumetric wear rates for the matrix and composites as a function of loads. ○ matrix; ⊕ average composites.

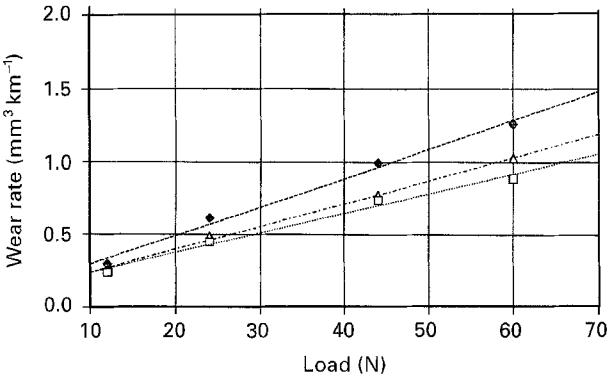

Figure 17 Average volumetric wear rates for N (□), P ⊕ and AP (△) orientations as a function of loads.

content, it may be concluded that the surface topography effects are dominant. The metallographic examination showed that in general the hard boron fibres protruded from the wear surfaces and bore the brunt of the load applied to the pin. Fracture of the fibres occurred as a result of this at and often below the sliding surface which resulted in a partial loss of fibres, and consequently of their support of the load, which in turn exposed the matrix to wear by spalling and ploughing, as in the unreinforced alloy. Broadly the more fibres present in the surface the lower were the loads on the matrix and the smaller the extent of matrix delamination and ploughing, but the wear mechanism remained essentially the same.

The effect of test piece orientation was to modify the effectiveness of the fibres in bearing the major part of the surface load. The effect on the wear rates was small in absolute terms, although the percentage changes could be very considerable due to their small absolute values. Fig. 1 showed that with the exception of the 16% fibre composite, the P orientation gave the highest, the AP intermediate and the N orientation the lowest wear rates under all conditions. For the 16% fibre composite the N orientation gave the highest wear rate at low loads, but the effect diminished with increased load and at 60 N it gave the lowest wear rate. Because the effect of fibre volume fraction was of secondary importance, the effect of orientation could be isolated by calculating the mean wear rates for the N, P and AP orientations from the data for all fibre contents, and the results are plotted against load in Fig. 17. This figure shows that the mean wear rates were linear functions of load, and that the P orientation composites wore at a significantly higher rate than the N and AP orientation composites, with the N orientation showing the lowest wear rates by a small margin.

The reasons for this effect of orientation must be due to different degrees of retention of fibres or fragments of fibres in the wear surface, which in turn must be related to the way that the fibres were loaded by the forces induced by compressive loading of the sliding surfaces.

Considering first the behaviour of the N orientation composites, it was found that the worn surface of the composites possessed a relatively smooth appearance with protruding fibres, as shown in Figs 3 and 4. In Fig. 4 and the cross-section micrograph of Fig. 11 it was observed that the flat ends of the fibres were chipped, the pieces of fibre averaging some 10 to 25 μm in length. Aluminium alloy has a lower elastic modulus than boron, so under compressive loading the elastic strain induced in the composite would produce a higher axial compressive stress in the fibres than the matrix. Wear of the surface also exposed the fibre ends so that the fibres would be end-loaded in compression as well as along the fibre length. During sliding wear, the frictional force produced a shear stress on the fibre ends parallel to the rubbing direction, which applied a bending moment to the fibres. The fibres then acted as very short, stiff cantilever beams supported by a low-modulus matrix which made fracture by bending less easy than fracture by chipping of the exposed edges of the cylindrical fibres. The lack of deep subsurface deformation also showed that the fibres in this orientation had been efficient strengtheners of the matrix. Low wear rates resulted from this combination of a low rate of fibre damage by chipping and a well-protected matrix, aided by the ability of the numerous protruding fibre ends to trap detached particles of the matrix alloy, which became smeared over them, and also small fibre fragments which would thus have been able to contribute a degree of wear-resistance to the surface.

In the P orientation fibre breakage occurred both in the surface and subsurface regions, producing many short segments of fibres, some of which had peeled away. Consideration of the stresses on an isotropic fibre lying parallel to the surface and subjected to an axial frictional force and radial compressive force, indicates that for a coefficient of friction of 0.6, a tensile stress equal to about one-third of the normal stress, would be set up acting at an angle of approximately 25° to the sliding direction. The fibre would be expected to fracture into segments with steeply angled fracture surfaces, and this prediction is partially confirmed by Fig. 7. A very significant finding of the microscopic examination was that following fracture of the continuous fibres into segments, some of these were pulled bodily out of the surface by the frictional forces on them, leaving large areas of predominantly matrix alloy exposed to more rapid wear. Fig. 12 confirmed deep subsurface damage in P orientation samples. In areas where the fibres were retained, many

wore down by abrasion but eventually shattered into small fragments. However, in contrast to the N orientation, few of these small fragments of fibres became embedded in the matrix as the sliding direction coincided with the direction of the surface grooves left by fibre loss, leading to low entrapment efficiency. The relatively high wear rates of the N orientation were thus determined by the combination of these adverse surface characteristics.

For the AP orientation, the frictional force acted normal to the fibre axes, tending to load them in bending. The metallographic examination showed that the fibres were broken up by the resulting axial tensile stresses into short fragments of irregular morphology, and even in the subsurface region fracture of the fibres had taken place. However, as the sliding direction was normal to the grooves left by detachment of pieces of fibre, these grooves acted as efficient traps for the wear debris, resulting in the retention of fibre fragments in the surface where they remained to contribute to wear resistance. The result was that the AP orientation was only marginally worse than the N orientation and significantly better than the P orientation in resisting dry sliding wear.

The coefficients of friction shown in Fig. 2 varied with fibre content and load in a much more complicated manner than the wear rates, and the differences between the fibre orientations were much more distinct, although the trends in behaviour were broadly similar. For the unreinforced matrix alloy, a modest decrease in coefficient of friction occurred for an increased load. This is commensurate with oxidative wear, in which the increased temperature caused by the higher load causes a film of oxidized debris to build up on the wear surface, which reduces the coefficient of friction. For the MMCs the behaviour was not so simple. All tended to have a peak in the friction coefficient versus fibre curve, which diminished in height and moved to lower values of fibre content as the test load increased. The N and P orientations had similar values of the coefficient of friction, but the peaks moved back to higher fibre contents when the load was increased from 44 to 60 N. The AP orientation gave higher values than the others, but the position of the peak remained at 23% at all loads except 44 N, when it was at 16% fibre. Comparison of the wear curves of Fig. 1 with the coefficient of friction curves of Fig. 2 showed a distinct inverse correlation of the graphs: high wear rates produced low coefficients of friction and vice versa.

To explore this in more detail, the mean wear rate for each orientation was calculated and plotted against the mean friction coefficient, and the resulting curves are shown in Fig. 18.

The P orientation differed from the others in that there was only the very slightest decrease in coefficient of friction with increased wear rate. This behaviour is immediately explained by the geometry of the fibres relative to the wear surface, and the metallographic examination of the surfaces. The counter-material in this case bore against long fibres lying in the surface, with the sliding direction aligned axially along the smooth surfaces of these fibres. During wear, parts of

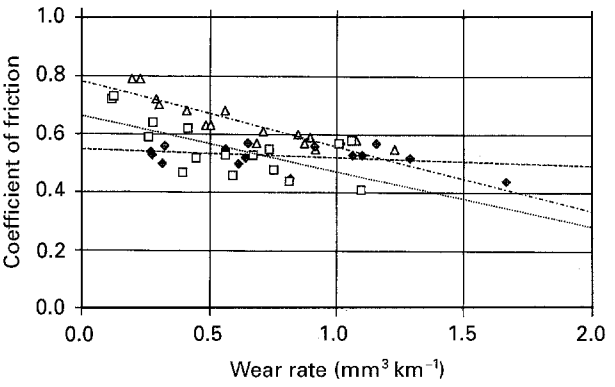

Figure 18 Average coefficient of friction versus wear rates for the different orientations of the composites. □ N; ◈ P; △ AP.

these fibres became detached and some were removed entirely from the surface by sliding out of their grooves, but in contrast to the other orientations even when the fibres were fragmented the small pieces of fibre were not embedded in the general surface. Thus the remaining fibres in the surface, and new fibres exposed by wear, continued to carry the compressive load on the wear pin whatever the rate of wear, and the sliding of the counter material along the mostly smooth surfaces of the embedded fibres in turn produced a nearly constant coefficient of friction.

The other orientations, with their more complex geometry, behaved quite differently. The AP orientation had higher mean values for the coefficient of friction, but the rate of decrease with increased wear rate was almost exactly the same for the N and AP orientations. This suggests that the increased friction of the MMCs compared with the matrix alloy was due to the abrasive action of hard fibres, and particles detached from fractured fibres and embedded in the matrix alloy, rubbing against the counter-material. For the N orientation the steel disc rubbed against the approximately flat ends of the protruding fibres of the composite, whereas for the AP orientation the disc rubbed against irregular particles of fractured fibres embedded into the surface of the pin, which gave a higher coefficient of friction. More fibres in the composite reduced the average compressive loads between the fibre and counter-material, which reduced the wear rate, but for a given load the increased number of contacts between the rubbing surfaces first increased the coefficient of friction then decreased it as the decreased compressive stress reduced the extent of fibre fracture.

The effect of load on the coefficient of friction was not so clear cut. In Fig. 18 the high-friction data points at low wear rates were from the low-load test conditions, since wear in the MMCs was insensitive to fibre content. To examine this relationship more clearly, the mean coefficients of friction for each composite orientation, and for the unreinforced matrix alloy, were calculated and are plotted against load in Fig. 19. This figure shows that with the exception of the P orientation, the MMCs emulated the load-dependence of the matrix alloy, but with higher base levels, suggesting that the matrix was responsible for this effect in the composites. It was shown in a

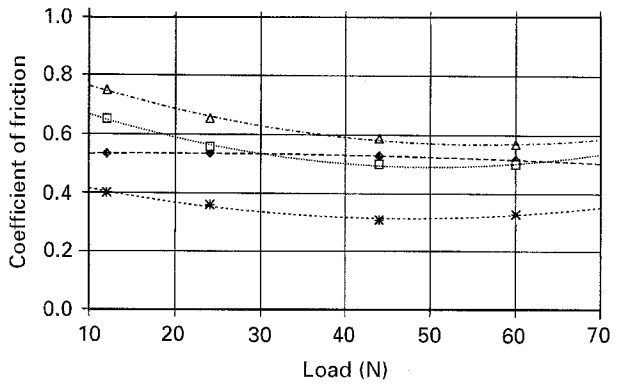

Figure 19 Average coefficient of friction versus applied loads for the matrix and different orientations of the composites. □ N; ◈ P; △ AP; * matrix.

previous study that in these composites and their matrix alloy oxidative wear took place with the formation of a complex surface layer on the wear surface [7]. Thus the effect of decreased load was possibly that lower temperatures reduced the rate of formation of the oxidized layer on the matrix in the composites, thus increasing the coefficient of friction, as in the case of the unreinforced matrix alloy.

5. Conclusions

1. Under the test conditions used for this work, the rate of dry sliding wear of aluminium alloy 2014 and B(SiC)/2014 composites increased linearly with load.

2. The average wear rate of the composites was 18% of that of the matrix for the same load, this constant proportion indicating that the mechanism of wear was similar in these materials.

3. Increase in fibre content of the MMCs in the range 16 to 23 vol % gave a very small reduction in wear rate, and further increases to 32 vol % had no regular effect.

4. The orientation of the fibres relative to the sliding surface and sliding direction had a small but significant effect on wear. The mean wear rates for each orientation were linear functions of load, with the P orientation composites wearing more rapidly than the N and AP orientations and the N orientation showing the lowest wear rates by a small margin.

5. The principal effect of orientation on wear rate was to modify the degree to which the fibres or fragments of fibres were removed from the wear surface of the pin.

6. The coefficients of friction of the MMCs were must higher than those of the unreinforced 2014 aluminium alloy, indicating that the abrasive action on the counter material of fibres or fragments of fibres in the wear surface of the pins was responsible for much of the friction.

7. The coefficients of friction of the N and AP orientated composites decreased linearly with increasing wear rate. The rate of decrease was almost exactly the same for the N and AP orientations, but the AP orientation had higher mean coefficients of friction.

8. The coefficients of friction of the N and AP orientated composites decreased non-linearly with increasing load in a similar way to that of the unreinforced matrix alloy. This is considered to be due to the increased formation of low friction surface films on the alloy matrix by oxidative wear under higher loads.

9. The coefficients of friction of the P orientation were almost independent of wear rate and of load due to the load being carried principally by long smooth fibres aligned parallel to the sliding direction.

References

1. M. M. SCHWARTZ, "Composite materials handbook" (McGraw-Hill, New York, 1984).
2. M. E. BUCK, *Materials and Design* **8** (1987) 272.
3. B. C. PAI, P. K. ROHATGI and S. VENKATESH, *Wear* **30** (1974) 117.
4. B. P. KRISHMAN, N. RAMAN, K. NARAYANASWAMI and P. K. ROHATGI, *ibid.* **60** (1980) 205.
5. T. L. HO and M. B. PETERSON, in "Wear of Materials", edited by N. A. Glasser and W. A. Glasser (ASME, New York, 1977) p. 70.
6. A. T. ALPAS and D. EMBURY, *Scripta Metall Mater.* **24** (1990) 931.
7. Y. SAHIN, Ph.D. Thesis, The University of Aston in Birmingham, 1994.
8. Y. SAHIN and S. MURPHY, *Wear* in press.
9. Z. ELIEZER, C. H. RAMAGE and M. F. AMATEAU, *Wear* **49** (1978) 119.
10. M. F. AMATEAU, W. W. FRENCH and D. M. GODDARD, in Proceedings of 1975 International Conference on Composite Materials, Vol 2 (TMS-AIME, New York, 1976) p. 623.
11. M. F. AMATEAU, R. H. FLOWERS and Z. ELIEZER, *Wear* **54** (1979) 175.
12. M. F. AMATEAU, in "Mechanical behaviour of metal matrix composites", edited by J. E. Hackaw and M. F. Amateau (TMS-AIME, Warrendale, PA, 1983) p. 213.
13. N. SAKA and N. K. SZETO, *Wear* **157** (1992) 339.
14. J. TAO, C. WANG and M. YING, in Wear of Materials 8th International Conference Orlando, edited by K. C. Ludema and R. G. Bayer (ASME, 1991) p. 601.
15. ASM Engineered Materials Reference Book, (ASME International, Metals Park, OH, 1989).
16. A. K. DHINGRA and L. B. GULBRANSEN (eds), in Proceedings of Cast Reinforced Metal Composites, Chicago, (1988) p. 179.
17. H. NAYEB-HASHEMI, J. T. BLUCHER and J. MIRAGEAS, *Wear* **150** (1991) 21.
18. H. FUKANAGA and I. SAKAI, in Proceedings of the 5th Conference on Production Engineering, Tokyo (1984) p. 673.
19. S. DAS and B. K. PRASAD, *Wear* **162–164** (1993) 64.
20. B. S. TRIPATHY and M. J. FUERY, *ibid.* **162–164** (1993) 385.
21. B. VISWANATH, A. P. VERMA and C. V. S. KAMESWARA RAO, *Composites* **21** (1990) 531.
22. P. K. ROHATGI and B. C. PAI, *Wear* **59** (1980) 323.

Received 10 August
and accepted 21 December 1995